

## HEAT AND MASS TRANSFER PROCESSES OF SOLID-STATE HYDROGEN DISCHARGING: A CFD STUDY

R. Meneceur<sup>1\*</sup>, A. Boukhari<sup>1,2</sup>, S. E. Laouini<sup>3</sup>, M. E. H. Attia<sup>2</sup>

<sup>1</sup>Department of Mechanical Engineering, Faculty of Technology, El-Oued University, Algeria

<sup>2</sup>Theory of Operators and PDE Laboratory, Faculty of Exact Sciences, El-Oued University,  
Algeria

<sup>3</sup>Department of Process Engineering and Petrochemicals, Faculty of Technology, El-Oued  
University, Algeria

Received: 07 November 2019 / Accepted: 10 April 2020 / Published online: 01 May 2020

### ABSTRACT

This article deals with the numerical simulation of a two-dimensional instantaneous heat and mass transfer processes within a commonly used intermetallic compound (a.k.a. Mischmetal) packed in a unit disc of an annulus-disc reactors, during hydrogen gas desorption. Using the finite volumes technique bundled in the OpenFOAM<sup>®</sup> CFD code, temperature and amount of desorbed hydrogen and their time-averaged quantities inside the metal-hydride packed bed are obtained for various temperatures of fluids used in heat transfer, and several outlet pressure magnitudes. Using a set of numerical simulations, we have emphasized the impacts of both parameters on metal-hydride reactor performance related to discharging time. An excellent accord was recorded for the present simulations results compared against the literature-reported experimental data [20].

**Keywords:** Metal hydride; LaNi<sub>5</sub>; Desorption; Numerical simulation; Finite volumes.

Author Correspondence, e-mail: [r.meneceur39@mail.com](mailto:r.meneceur39@mail.com)

doi: <http://dx.doi.org/10.4314/jfas.v12i2.9>



## 1. INTRODUCTION

The fact of viewing hydrogen as a universal energy carrier among various clean alternative energy sources, makes it worthy of extensive consideration in the scientific researches field, because its richness in nature and diversity of its primary energy sources that can be able to reproduce it; including sustainable resources such as solar, wind and biomasses, besides the currently exploited alternatives such as fossil energy and nuclear power. Furthermore, its use in fuel cells produces water as a side effect, the latter being a nature-friendly product, which makes this energy alternative (hydrogen energy) environmentally safe and inexpensively beneficial in the chart of its industrial exploitation [1,2].

Nevertheless, for many practical applications, the use of hydrogen-based fuels is limited by various restrictions ranging between transportation and storing problems. In the recent years, a diversity of techniques for hydrogen storage has been industrialized for this reason. Among these technologies, one can mention the solid-state hydrogen reversible storage technique, where it is stored as metal hydrides using intermetallic compounds, carbon or on composite materials so-called multi-wall carbon nanotubes (MWCNTs) [3]. Above and beyond the security and its lower cost, the latter storage technique using metal hydrides have attracted substantial attention, owed to their relatively higher volumetric density compared to that issued from liquid hydrogen techniques, but a low hydrogen absorption capacity came into sight [1]. Plentiful industrial applications require a lower hydrogen quantity compared to others. Yet, in addition to their disadvantage of weight, metal hydrides-based hydrogen storage have another disadvantage which is their bounded kinetics, since they deal with huge quantities of heat through the sorption processes, and the hydrogen sorption rate is limited by the resulting metal thermal properties. This fact causes severe confronts to the thermal management of those exchanged heat amounts during sorption processes [4]. A certain measure of metal-hydrides-based storage systems performances is the rates of hydrogen sorption process, which depends on the rate of reaction heat delivery or removal from the considered handled system. For this reason, the metal hydride (MH) reactors thermal management comes across complex phenomena of coupled (i.e. simultaneous) heat and mass transfers in absorbent packed beds where all the three heat transfer modes take place

concurrently.

The obvious dependency of H<sub>2</sub> gas sorption rates on heat transfer characteristics and reaction kinetics of the MH packed beds were argued by the literature [4,5]. Characteristics of the occurring simultaneous heat and mass transfers phenomena in hydride beds during H<sub>2</sub> sorption processes have been considered in numerous investigations, using a diversity of mathematical models; ranging from those having one dimension and focusing primarily on heat conduction [6], to those considering convection side by side to thermal conduction [7] followed by those combining the conduction, convection and thermal radiation effects [8,10-11]. Other configurations had been studied in the geometrical framework notoriously; the two-dimensional models of the works [8-11], and the illustrious three-dimensional model present in the studies of Aldas et al. [4]. Several carried out works [8-10] led to the conclusion that thermal radiation effects on sorption process are insignificant in case of LaNi<sub>5</sub>-based hydrogen storage devices (i.e. low-temperature hydrides), and are significant for the Mg-based hydrogen storage devices (i.e. high-temperature hydrides), regardless of the fact that convection effects are substantial and crucially influences the temperature field, however the overall metal-hydride formation is found to be not influenced by the fluid movement.

Dogan et al. [12] studied the MH-based hydrogen store behavior numerically, and they found that temperature increases unfavorably affect the absorption rate. Therefore the system should be efficiently cooled for a fast charging. Also, they investigated the impact of two charging systems on filling time and found that hydrogen gas must be supplied radially to obtain rapid H<sub>2</sub> filling.

The development and design processes of thermal energy exchangers require the exploitation of the Computational Fluid Dynamics (CFD) methods. Principally, while investigating instantaneous heat and mass transfer processes in porous media, e.g. reactors consisting of packed beds employed in energy storage systems, or in the fuel cells modeling and design [13]. Mitsutake et al. [14] proposed and investigated the fact of improving the heat transfer by conduction and hydrogen absorption using radial and circular fins in a cylindrical hydrogen stowage tank filled with La-Ni-based MH alloy. They verified a simple reaction model by comparison with experimental results, and predicted hydrogen absorption times for a broad

---

range of conditions aiming to provide the optimum fin layout. Although, some researches tried to inspect the operation of heat and mass transfers inside the adsorption bed in a solid adsorption refrigeration system, by establishing some mathematical models, then solving them numerically [15]. Later, Krokos et al. [16] presented an original approach for the design optimization of a sort of multi-tubular MH storage tank, equipped with up to 9 tubular MH reactors, used in on-board applications involving hydrogen storage techniques. They numerically investigated the cooling tubes arrangement inside the packed bed, and found that a regular cooling tubes configuration yielded an optimal end-result in accord to their meticulous 3D Cartesian mathematical model. Simultaneously, Freni et al. [17] concluded that a shorter refueling time would be obtained at higher heat exchange rate after studying numerically a symmetrically embedded cooling tube within the reaction bed. They performed numerical computations to demonstrate that increasing the hydride thermal conductivity can further enhance the reactor dynamical performances, in case of sufficiently permeable absorbent bed to hydrogen.

However, the aforementioned research works or models have ignored the plateau slope attribute of the pressure-concentration isotherms (PCI) associated to the working alloy, as well as its hysteresis parameter while reaction cycles. Consequently, the main persistence of the present work is to investigate numerically the heat and mass transfer simultaneous processes, occurring during H<sub>2</sub>-sorption of in a reactor unit of type annulus-disc (ADR) containing LaNi<sub>5</sub> intermetallic compound. A practical configuration of an ADR would involve many annular discs to provide hydrogen gas, which is desorbed from the MH packed bed, and flowing into the inner tube. In this paper, the simulation was achieved by the application of finite volume technique bundled in the general-purpose CFD code OpenFOAM (considered as open source) to resolve the mathematical models describing such a device operation containing LaNi<sub>5</sub> as the dehydrating metal.

Numerical calculations for the present investigation were carried out through the adoption of the famous two-dimensional mathematical model of Demircan et al. [8], aiming to examine and clarify the heating fluid temperature and the H<sub>2</sub> gas delivery-pressure effects on dynamical performances of the considered MH reactor system.

## 2. MATHEMATICAL MODEL AND SOLUTION TECHNIQUE

At present, the considered mathematical model describing the annulus-disc reactor (represented in Figure 1.a) is akin to that present in the works of Demircan et al. [8], with the  $\text{LaNi}_5\text{-H}_6$  as the dehydriding solid, which is filling the annular space between the inner central  $\text{H}_2$ -delivery tube and the outer peripheral heating wall. A number of embedded heating tubes crosses the annulus disc unit in that case of hydrogen desorption process. For the reason of angular periodicity, we will restrict the computational domain to half of the sector area between two adjacent heating tubes. In the current work, the thermo–physical properties of  $\text{H}_2$  gas, and the working alloy adopted are those frequently used in literature [9-11, 20, 23]. The computational domain and the used mesh grid where seen on Figure 1.b. The unit of the ADR reactors comprises two phases; a solid phase i.e. the hydride alloy, and a gaseous phase i.e.  $\text{H}_2$ , consequently, a porous medium formation will take place.

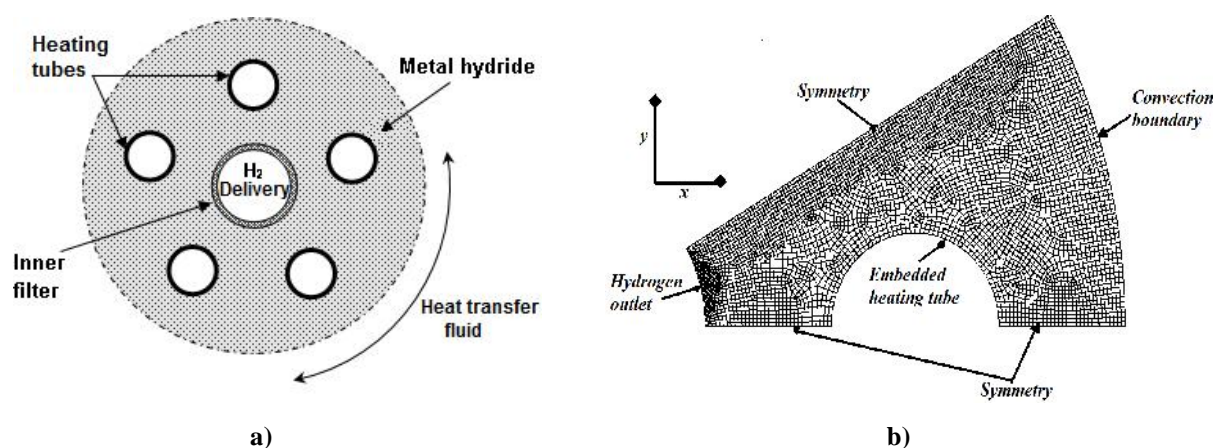


**Fig.1. a)** Schematic sliced view of the studied ADR unit disc equipped with isothermal heating tubes, and **b)** ADR unit portion with the prescribed boundary conditions, and its computational mesh

Generally, the simplifying hypotheses considered while applying the present mathematical model are the following:

1. The gas phase is ideal from a thermodynamic viewpoint.
2. Porosity is uniform and its variation with desorption is negligible.

3. Mass transfer process takes place through the porous filter (H<sub>2</sub> delivery), in addition to the constantly maintained hydrogen outlet pressure and temperature.
4. The temperature field is identical for gas and solid phases (local thermal equilibrium hypothesis) in this porous medium, even though radiative thermal energy transfer is negligible.
5. The radial temperature gradient within the heating tubes is negligible; consequently they are considered isothermal tubes.

## 2.1 Volume-Averaged Governing Equations

The additional source term included in the RHS of the mass conservation equation, denote the hydrogen amount flowing from the bed with time;

$$v \frac{\partial \dots_g}{\partial t} + \vec{\nabla} \cdot (\dots_g \vec{V}) = \dot{m} \quad (1)$$

and here denote hydrogen quantity that is out-flowing from the solid with time;

$$(1-v) \frac{\partial \dots_s}{\partial t} = -\dot{m} \quad (2)$$

The perfect gas state equation states that;

$$P = \frac{R_g}{M_{H_2}} \dots_g T \quad (3)$$

where  $R_g$  and  $M_{H_2}$  stand for the universal gas constant, and hydrogen gas molecular weight, respectively.

By taking into consideration the Forchheimer modification term in momentum (i.e. Navier-Stokes) equations, we have;

$$\frac{\dots_g}{v} \left[ \frac{\partial \vec{V}}{\partial t} + \vec{V} \cdot \vec{\nabla} \left( \frac{\vec{V}}{v} \right) \right] = -\vec{\nabla} \cdot P + \frac{\sim}{v \dots_g} (\Delta \vec{V}) + S_D \quad (4)$$

where  $S_D = - \left[ \frac{\sim}{K} + \frac{1.75 \dots_g}{\sqrt{150 K v^3}} |\vec{V}| \right] \vec{V}$  represent the source term instead of the additional pressure within the packed bed owed to viscous effects. In these equations  $|\vec{V}|$  is the gas flow velocity magnitude, where  $K$  and  $v$  are the permeability, and the porosity of this porous medium (i.e. the packed bed) [19].

The equation of energy in the MH packed bed can be stated using a single temperature variation;

$$\left[ v \dots_g C_{pg} + (1-v) \dots_s C_{ps} \right] \frac{\partial T}{\partial t} + (\dots_g C_{pg} \vec{V}) \vec{\nabla} T = \vec{\nabla} \cdot \left[ (v \dots_g + (1-v) \dots_s) \vec{\nabla} T \right] - \dot{m} [\Delta H - T (C_{pg} - C_{ps})] \quad (5)$$

## 2.2 Reaction Kinetics

The amount of hydrogen gas that is desorbed from the metal with respect to time has been directly linked to the dehydrogening process reaction rate; the latter is conveyed as in [8]:

$$\dot{m} = C_d \exp\left(-\frac{E_d}{R_g T}\right) \left[ \frac{P - P_{eq}}{P_{eq}} \right] [\dots_s - \dots_0] \quad (6)$$

where  $C_d$  is a material-dependent absorption rate constant,  $E_d$  is the activation energy,  $\dots_0$  is the H<sub>2</sub>-free MH density, and  $P_{eq}$  is the equilibrium pressure obtained from the van't Hoff relationship

$$P_{eq} = P_0 \exp\left(A - \frac{B}{T} + w_{slp} (\langle - \langle_0 \rangle) + w_{hys}\right) \quad (7)$$

where  $w_{slp}$  is the slope factor of the plateau pressure in the sorption PCI of LaNi<sub>5</sub> alloy, and  $w_{hys}$  is its hysteresis factor,  $P_0$  is the reference pressure (1 atmos),  $A$  and  $B$  are van't Hoff constants [21].

## 2.3 Initial and Boundary Specified Conditions

At the initial time  $t = 0$ ;  $P(x, y, 0) = P_0$ ,  $T(x, y, 0) = T_0$ ,  $\dots_s(x, y, 0) = \dots_{s,0}$ .

And later for  $t > 0$ ;

- At the delivery hydrogen gas (i.e. the central tube);  $P = P_0$ ,  $T = T_0$ .
- The lateral heating wall (Figure 1.b) :

$$-\left(v \dots_g + (1-v) \dots_s\right) \frac{\partial T}{\partial \vec{n}} = h(T - T_f) \quad (8)$$

where  $h$  is the conductance between the MH packed bed and the heating fluid (HTF) at temperature  $T_f$ , taken from the work of Ben Nasrallah [20], and  $\vec{n}$  is the normal unit vector outwarding the boundary.

- The embedded heating tubes, which are assumed to be isothermal (Figure 1.b), having the value  $T = T_f$ .
- The symmetry condition type is type where assumed to prevail in all other boundaries.

## 2.4 Solution Technique

The model governing equations were solved after discretization via the finite volume technique bundled in the OpenFOAM<sup>®</sup> code, which is an industrial purpose open source package. The technique to obtain numerical solution consists of expressing the model governing differential equations via a set of general algebraic equations, then to integrate those numerically over the finite volume-meshed computational domain exposed in Figure 1.b.

The aforesaid general algebraic form of transport equation is written as [22]:

$$\frac{\partial(\dots)}{\partial t} + \vec{\nabla} \cdot (\dots \vec{V} \{ \}) = \vec{\nabla} \cdot (\Gamma \vec{\nabla} \{ \}) + S_c \quad (9)$$

where  $\{$  refer to a certain generic transported physical quantity (the field variable),  $\Gamma$  is the coefficient of diffusion and  $S_c$  is all source terms. Whilst, the pressure-velocity coupling is solved by invoking the solver called buoyantBoussinesqPimpleFoam, which consists of a kind of large time-step transient solver for incompressible, buoyant porous media flows using the PIMPLE (a merged PISO-SIMPLE version) algorithm [22, 24]. Although, the presented in Figure 2 lay emphasis on the main steps taken by this numerical technique. Calculations were carried out on a Core™ i3 PC, taking about 5 hours per a typical case, and using some parallelization features present in the aforementioned CFD code (i.e. OpenFOAM). Also, we have introduced a certain form of the volume-weighted average discrete formula (a kind of arithmetic mean) to compute the value of some variable quantities, in the aim to attain a coherent measure of the performance assessment of metal hydride reactors of this type [24].



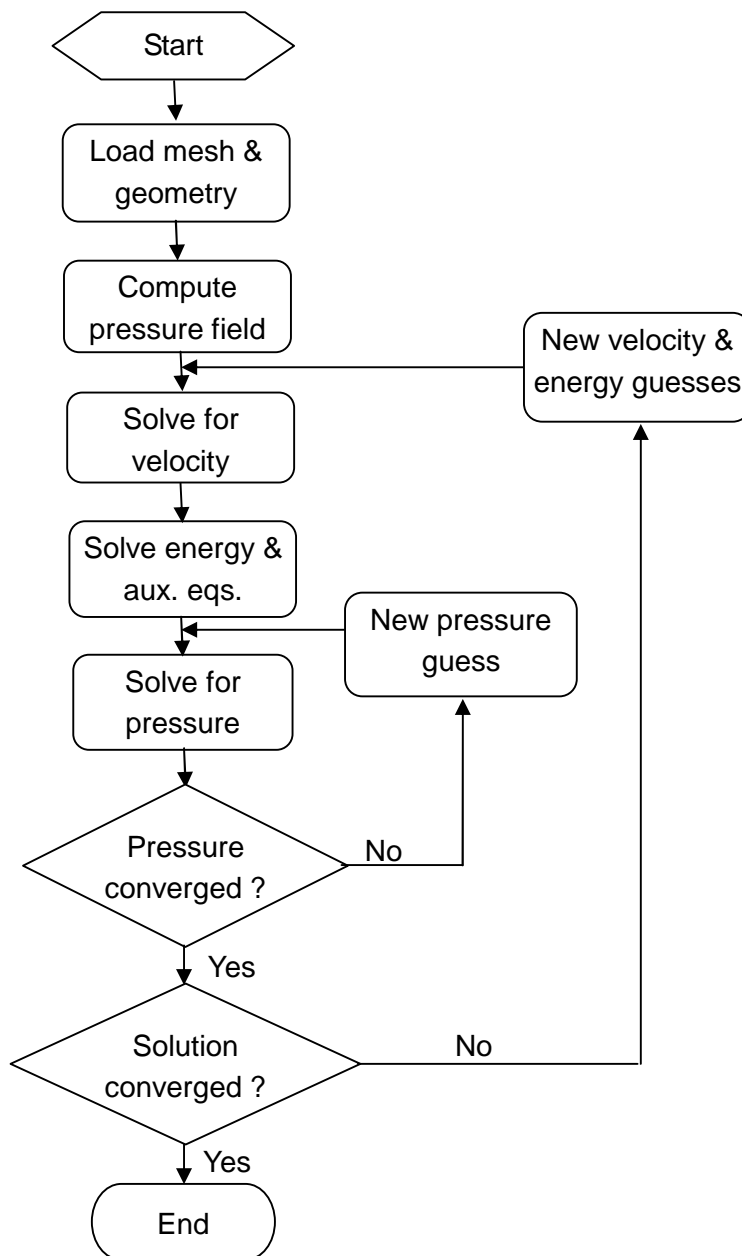


**Fig.2.** The PIMPLE algorithm flowchart

### 3. RESULTS AND DISCUSSION

#### 3.1 Grid Independency Tests

After the mathematical model being established, a mesh independency tests were performed to examine the impact of the computational grid (mesh) on the average reacted fraction versus time. The numerical solution behavior is tested against a group of four mesh grids, which gives a variety of mesh sizes, ranging from 3910, 4229 and 4744 up to 8697 quadrilateral Cartesian cells, as detailed on Table 1.

**Table 1.** Sizes and attributes of different mesh grids used in the mesh independency tests

Grid case	Mesh size	Mesh attributes	
		min. cell area ( $m^2$ )	max. cell area ( $m^2$ )
A	3910 quadrilateral cells, 7990 faces	$1.3442 \times 10^{-7}$	$6.3478 \times 10^{-6}$
B	4229 quadrilateral cells, 8638 faces	$6.6040 \times 10^{-8}$	$5.9413 \times 10^{-6}$
C	4744 quadrilateral cells, 9675 faces	$9.3107 \times 10^{-8}$	$6.0009 \times 10^{-6}$
D	8697 quadrilateral cells, 17654 faces	$1.4244 \times 10^{-8}$	$3.5961 \times 10^{-6}$

As clarified in Figure 3, a very close accord is observed between several tested computational meshes. That's why the present simulations will henceforth be carried out using the medium mesh (case C) having 4744 quadrilateral cells, which grants to us a moderate calculation times with ample precisions.

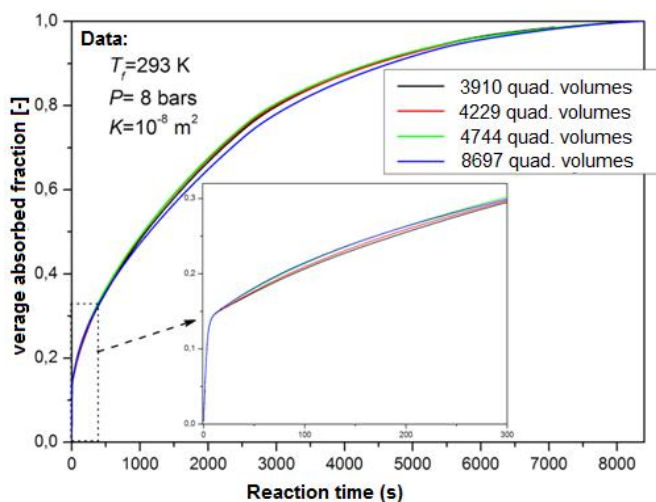


**Fig.3.** Mesh independence test on the transient compartment of the average H<sub>2</sub>-absorbed fraction

### 3.2 Numerical Results Validation

We have carried out numerous simulations in aim to validate the considered mathematical model, by comparison of the results with some experimental data figuring in the literature, namely the data from the work of Jemni et al. [20] wherein the authors have investigated a cylindrical shaped MH reactor containing the LaNi<sub>5</sub>-H<sub>2</sub> hydride. Additionally, we have intent

to apply the adopted 2D approach by assuming axial symmetry. Figure 4 shows the temperature history inside the metal hydride reactor at three selected points within it. Heating fluid temperature and delivery pressure were  $T_f = 20^\circ\text{C}$  and  $P = 8\text{bars}$  for this case, respectively. We can see at the early beginning of desorption process that the monitoring temperatures show a rushed decrease in the metal hydride packed bed, because the dehydrating reaction (i.e.  $\text{H}_2$  gas release) is endothermic, then increase progressively in an exponential growth, that can be owed to the van't Hoff's character of the reaction kinetics. These simulation results showed a good agreement judged against the considered experiments, divulging that the adopted model could be used for further examination of the dynamical performances of MH reactors.

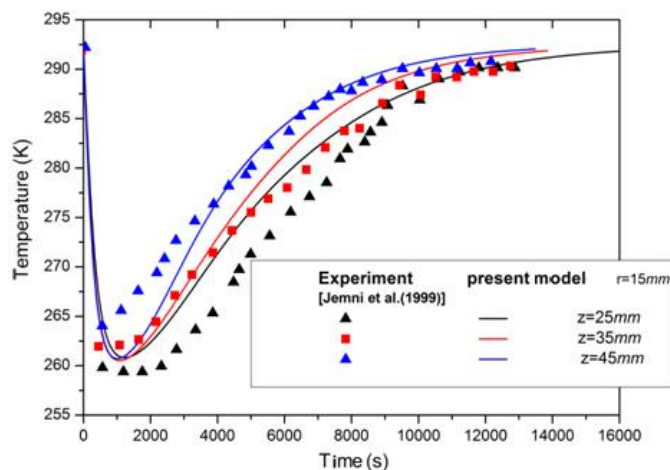


**Fig.4.** Temperature growth at selected points within a cylindrical-shaped  $\text{H}_2$  storage tank experimentally tested in [20] for the hydriding case (absorption) with HTF at  $20^\circ\text{C}$

### 3.3 Hydrogen Desorption From the $\text{LaNi}_5\text{-H}_6$ Alloy

In this section, we concentrate our attention on emphasizing the impacts of HTF temperature, and metal alloy thermal conductivity on  $\text{H}_2$  gas desorption inside the ADR-type MH reactor. Thus, heat and mass transfers dynamical behavior inside the annulus-disc reactor is inspected through a good number of numerical simulations centering attention on packed beds containing the intermetallic compound  $\text{LaNi}_5$ , considered as hydrogen-saturated ( $\text{LaNi}_5\text{H}_6$ ) porous material. This  $\text{AB}_5$ -type alloy, which present equilibrium pressures near atmospheric conditions at the ambient temperature, and can stock up to 1.42 wt% reversibly. Desorption

numerical simulations mentioned in the current work were carried at constant discharging pressure of  $P = 1$  bar, and at temperature of  $20$  °C. Simulations are realized for a temperature range of the heat transfer fluid as;  $T_f = 20^\circ, 25^\circ, 30^\circ$  and  $35^\circ\text{C}$ , in the aim to inspect the heating temperature influence on the desorption operation time of hydrogen gas stored in the solid (i.e. metal hydride). Delivery pressure effects on MH storage tank performance versus discharging times, and related  $\text{H}_2$  desorbed fraction, were examined by mean of a number of numerical simulations ranging in the interval;  $P = 0.1, 0.5, 1, 1.5,$  and  $2$  bars.

### 3.3.1 HTF Temperature Effects

Initially, the system is discharging its amount of stored  $\text{H}_2$  gas at an outlet pressure of  $1$  bar and outlet gas temperature of  $20^\circ\text{C}$ . The corresponding hydrogen concentration is  $1.44$  wt%. Figure 5 shows the progressive evolution of averaged temperature of the studied alloy contained in the porous packed bed. Hence, the augmentation of HTF temperature reduces visibly the discharging time of the  $\text{H}_2$  gas. Consequently, the heating temperatures affect positively (i.e. enhances) the examined MH storage tank performance while desorption.

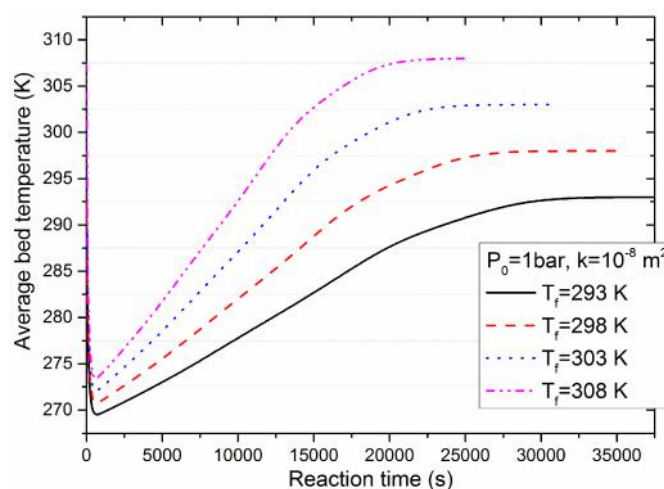


**Fig.5.** Time-based evolution of averaged temperature within the MH packed bed, where  $\text{LaNi}_5\text{-H}_6$  is the dehydriding solid

From the Figure 5, we observe also that the required time to attain the limiting value of average temperature is considerably impacted by the HTF temperature. Thus high heating temperatures led to high desorption rate, and consequently short discharging times. This fact is owed to the endothermic character of the desorption reaction.

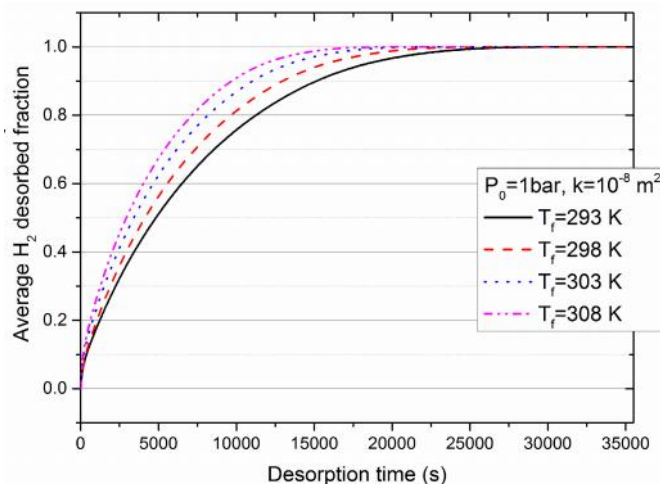


**Fig.6.** HTF temperature effect on H<sub>2</sub> gas desorption at constant discharging pressure

Figure 6 showing the temporal evolution curves of the bed-averaged desorption fraction of hydrogen gas, confirms our conclusion that the heating temperature augmentation is a favorable parameter in the metal hydride reactor desorption performance. The average desorbed fraction plots demonstrate that a complete desorption takes a delay of 5.55 hr in the case of heating fluid temperature of 20 °C. Nevertheless, the same bed-averaged fraction requires only about 4 hr and 10 min to be completely desorbed from the hydride in case of HTF temperature  $T_f=35^{\circ}\text{C}$ , which represents about 25% of reaction time reduction.

### 3.3.2 Delivery Pressure Effect on Discharging Time

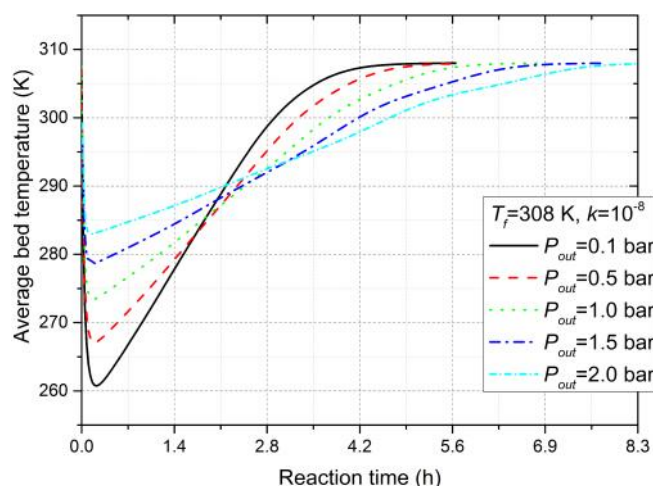


**Fig.7.** Average bed temperature evolution for the packed bed reactor heated at  $T_f=35^{\circ}\text{C}$

Figure 7 shows that increasing delivery pressure corresponds to an increase in desorption time.

In other terms, delivery pressure affects adversely the storage tank reactor performance, which led in turn to conclude that higher outlet pressure value could not be expected while optimizing the metal hydride reactor design.

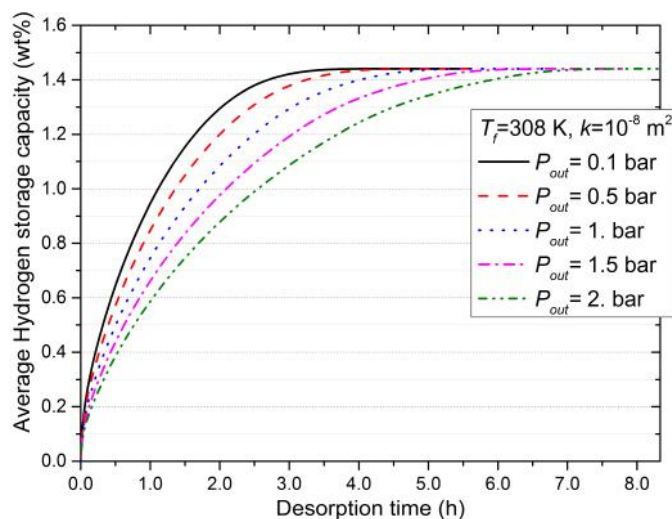


**Fig.8.** History of averaged H<sub>2</sub> storage capacity in wt% within a MH reactor at  $T_f=35^{\circ}\text{C}$

Figure 8 illustrates the dependence between delivery pressure and H<sub>2</sub> storage capacity, and in turn confirms the previous conclusion claiming that increasing the hydrogen gas outlet pressure (the delivery pressure) affects adversely the desorption times, thus the conclusion that the delivery pressure is not a key factor in the metal hydride reactor performance enhancement.

#### 4. CONCLUSION

A 2D mathematical model describing the transient simultaneous heat and mass transfers in packed metal hydride bed during H<sub>2</sub> gas desorption has been adopted. Where, the hydrogen desorption in its considered storage packed bed is investigated numerically in a packed unit of an annulus-disc reactor configuration. Calculations were performed by means of the finite volume numerical technique packaged in the CFD code OpenFOAM. The simulations results showed a good agreement in comparison against experimental data stated in the literature works. Because of investigating the heat exchange fluid temperature effects on discharging time, simulations results illustrates that high HTF temperatures led to significant improvement in reaction time, which makes it a key factor in MH reactors design and optimization. Also

within the present work, we have inspected the delivery pressure influence on desorption time, which was proven to adversely affect the discharging time.

## NOMENCLATURE

$C_d$	desorption rate coefficient, $s^{-1}$	<b>Greek symbols</b>	
$C_p$	specific heat, J/kg.K	$\Delta H$	heat of formation, J/kg
$E_d$	desorption activation energy, J/mol	$\}$	thermal conductivity, W/m.K
$h$	heat convection coefficient, W/m <sup>2</sup> .K	$\nu$	porosity
$K$	permeability, m <sup>2</sup>	$\sim$	dynamic viscosity, kg/m.s
$M_{H_2}$	hydrogen molecular mass, kg/kmol	$\dots$	density, kg/m <sup>3</sup>
$\dot{m}$	mass reaction rate, kg/m <sup>3</sup> s	$W_{slp}$	slope factor
$P$	pressure, Pa	$W_{hys}$	hysteresis factor
$R_g$	universal gas constant, J/mol.K	$\langle$	reacted fraction
$S_D$	Forchheimer's term		
$T$	temperature, K	<b>subscripts</b>	
$t$	time, s	0	initial
$\vec{V}$	velocity within the metal bed, m/s	$eq$	equilibrium
$wt\%$	hydrogen gas storage capacity	$f$	bath fluid
$x, y$	$x$ and $y$ -Cartesian system coordinates	$g$	gas
		$s$	solid

## 5. REFERENCES

- [1] Osumi Y. Hydrogen absorbing alloys. Agune Gijutsu Center, 1993
- [2] Heung L K. Using metal hydride to store hydrogen. DOE report, 2003, WSRC-MS-2003-00172
- [3] Noroozi A H, Safa S, Azimirad R, Shirzadi H R, and Yazdi N G. Microstructure and Hydrogen Storage Properties of LaNi<sub>5</sub>-Multi Wall Carbon Nanotubes (MWCNTs) Composite. Arab J. Sci. Eng., 2013, 38, 187–194
- [4] Aldas K, Mat M D, and Kaplan Y. A three-dimensional mathematical model for hydrogen absorption in a metal hydride bed. Int. J. Hydrogen Energy, 2002, 27, 1049-1056

- 
- [5] Minko K B, Artemov V I, and Yan'kov G G. Numerical simulation of sorption/desorption processes in metal-hydride systems for hydrogen storage and purification Part I: Development of a mathematical model. *Int. J. Heat Mass Transfer*, 2014, 68, 683-692
- [6] Gopal R, Murthy S. Prediction of heat and mass transfer in annular cylindrical metal hydride beds. *Int. J. Hydrogen Energy*, 1992, 17, 795-805
- [7] Amphlett J C. A heat transfer-based dynamic model for predicting charge and discharge rates of metal hydride systems. *Hydrogen Energy Prog.*, 1996, 11(3), 2711–2719
- [8] Demircan A, Demiralp M, Kaplan Y, Mat M D, and Veziroglu T N. Experimental and theoretical analysis of H<sub>2</sub> absorption in LaNi<sub>5</sub>-H<sub>2</sub> reactors. *Int. J. Hydrogen Energy*, 2005, 30, 1437-1446
- [9] Boukhari A, Bessaïh R. Numerical heat and mass transfer investigation of hydrogen absorption in an annulus-disc reactor. *Int. J. Hydrogen Energy*, 2015, 40, 13708-13717
- [10] Bouzgarrou F, Askri F, Ben Nasrallah S. Numerical Investigation of Heat and Mass Transfer During the Desorption Process of a LaNi<sub>5</sub>-H<sub>2</sub> Reactor. *J. Heat Transfer*, 2016, 138, 1-7
- [11] Chibani A, Bougriou C. Effect of the tank geometry on the storage and destocking of hydrogen on metal hydride (LaNi<sub>5</sub>H<sub>2</sub>). *Int. J. Hydrogen Energy*, 2017, 42(36), 23035-23044
- [12] Dogan A, Kaplan Y, and Veziroglu T N. Numerical investigation of heat and mass transfer in a metal hydride bed. *App. Math. Computation*, 2004, 150, 169-180
- [13] Visaria M, Mudawar I. Experimental investigation and theoretical modeling of dehydrating process in high-pressure metal hydride hydrogen storage systems. *Int. J. Hydrogen Energy*, 2012, 37, 5735-49
- [14] Mitsutake Y, Monde M, Shigetaka K, Tsunokake S, and Fuura T. Enhancement of Heat Transfer in Hydrogen Storage Tank with Hydrogen Absorbing Alloy (Optimum Fin Layout). *Heat Transfer—Asian Research*, 2008, 37(3), 165-183
- [15] Yang P. Mathematics Model for Heat and Mass Transfer on an Adsorption Bed. *Heat Transfer—Asian Research*, 2009, 38(8), 548-556
- [16] Krokos C A, Nikolic D, Kikkinides E S, Georgiadis M C, and Stubos A K. Modelling and optimization of multi-tubular metal hydride beds for efficient hydrogen storage. *Int. J. Hydrogen Energy*, 2009, 34, 9128-9140
- [17] Freni A, Cipiti F, and Cacciola G. Finite element-based simulation of a metal hydride-based hydrogen storage tank. *Int. J. Hydrogen Energy*, 2009, 34, 8574-8582



- 
- [18] Yang F, Meng X, Deng J, Wang Y, and Zhang Z. Identifying heat and mass transfer characteristics of metal hydride reactor during adsorption- parameter analysis and numerical study. *Int. J. Hydrogen Energy*, 2008, 33, 1014-1022
- [19] Bejan A. *Convection Heat Transfer*. 4<sup>th</sup> edn. John Wiley & Sons, Inc., New Jersey, 2013
- [20] Jemni A, Ben Nasrallah S, and Lamloumi J. Experimental and theoretical study of a metal–hydrogen reactor. *Int. J. Hydrogen Energy*, 1999, 24, 631-44
- [21] Sandrock G, Thomas G. IEA/DOE/SNL Hydride Databases, <http://hydpark.ca.sandia.gov>, Accessed 23 January 2012
- [22] Versteeg H K, Malalasekera W. *An Introduction to Computational Fluid Dynamics: the finite volume method*. 2<sup>nd</sup> edn, Pearson Education Ltd., 2007
- [23] Chibani A, Bougriou C, and Merouani S. Simulation of hydrogen absorption/desorption on metal hydride LaNi<sub>5</sub>-H<sub>2</sub>: mass and heat transfer. *Appl. Thermal Eng.*, 2018, 142, 110-117
- [24] OpenFOAM. *The Open Source CFD Toolbox User Guide*. Version v1606+, OpenCFD Ltd., 2016

**How to cite this article:**

Meneceur R, Boukhari A, Laouini SE, Attia MEH. Heat and Mass Transfer Processes of Solid-State Hydrogen Discharging: A CFD Study. *J. Fundam. Appl. Sci.*, 2020, 12(2), 650-666.